

**Improved performance of UV-blue dual-band Bi<sub>2</sub>O<sub>3</sub>/TiO<sub>2</sub>  
photodetector and application of visible light communication with  
UV light encryption**

Qin Zheng,<sup>a</sup> Jianping Xu,<sup>\*a</sup> Shaobo Shi,<sup>b</sup> Jing Chen,<sup>c</sup> Jianghua Xu,<sup>c</sup> Lina Kong,<sup>c</sup>  
Xiaosong Zhang,<sup>c</sup> and Lan Li<sup>b</sup>

<sup>a</sup>*Tianjin Key Laboratory of Quantum Optics and Intelligent Photonics, School of Science, Tianjin University of Technology, Tianjin 300384, China*

<sup>b</sup>*School of Science, Tianjin University of Technology and Education, Tianjin 300222, China*

<sup>c</sup>*School of Materials Science and Engineering, Key Laboratory of Display Materials and Photoelectric Devices, Ministry of Education, and Tianjin Key Laboratory for Photoelectric Materials and Devices, Tianjin University of Technology, Tianjin 300384, China*

*\*Corresponding author. E-mail addresses: xjp0335@163.com (J. Xu).*

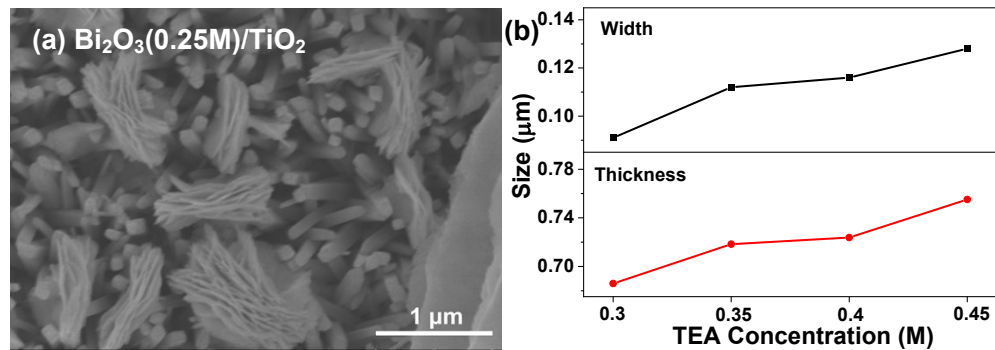


**Fig.S1** (a) SEM image of  $\text{Bi}_2\text{O}_3(0.25\text{M})/\text{TiO}_2$  and (b) lateral dimension and thickness of individual  $\text{Bi}_2\text{O}_3/\text{TiO}_2$  nanosheets with different TEA concentrations.

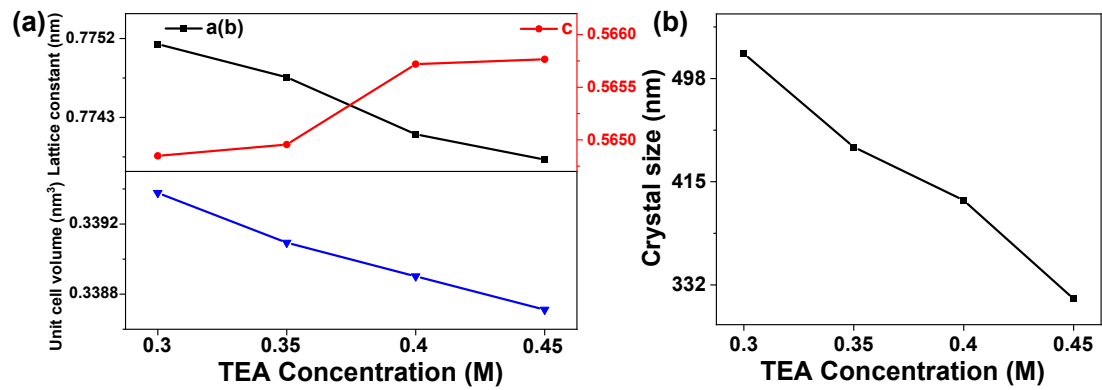


**Fig.S2** (a) Lattice constants and crystal volume, and (b) crystal size of  $\text{Bi}_2\text{O}_3/\text{TiO}_2$  with different TEA concentrations.

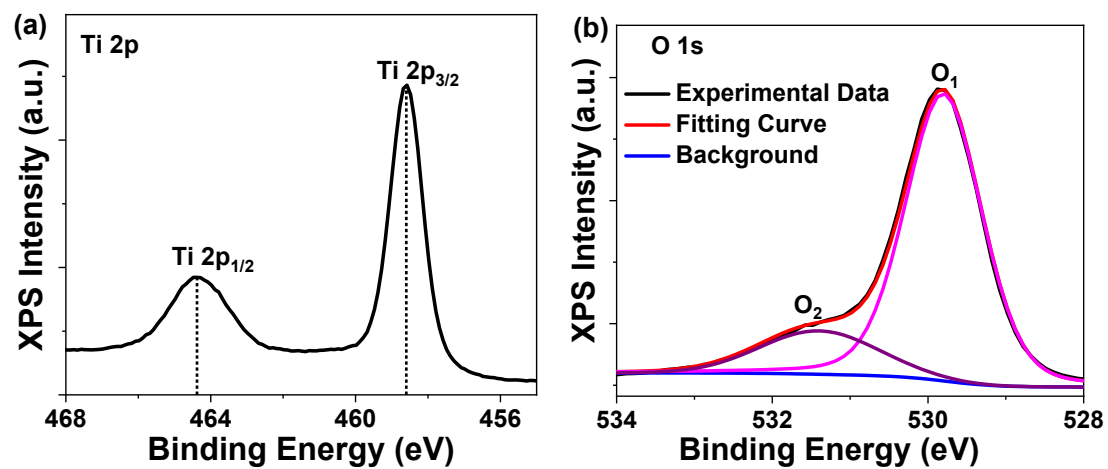


**Fig.S3** (a) Ti 2p and (b) O 1s XPS spectra of TiO<sub>2</sub> NRs.

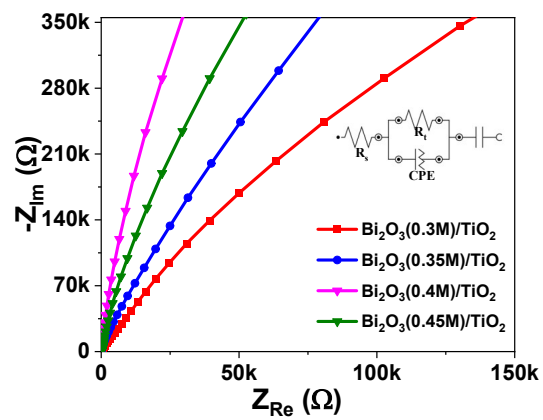


**Fig.S4** EIS curves of  $\text{Bi}_2\text{O}_3/\text{TiO}_2$  with different TEA concentrations.

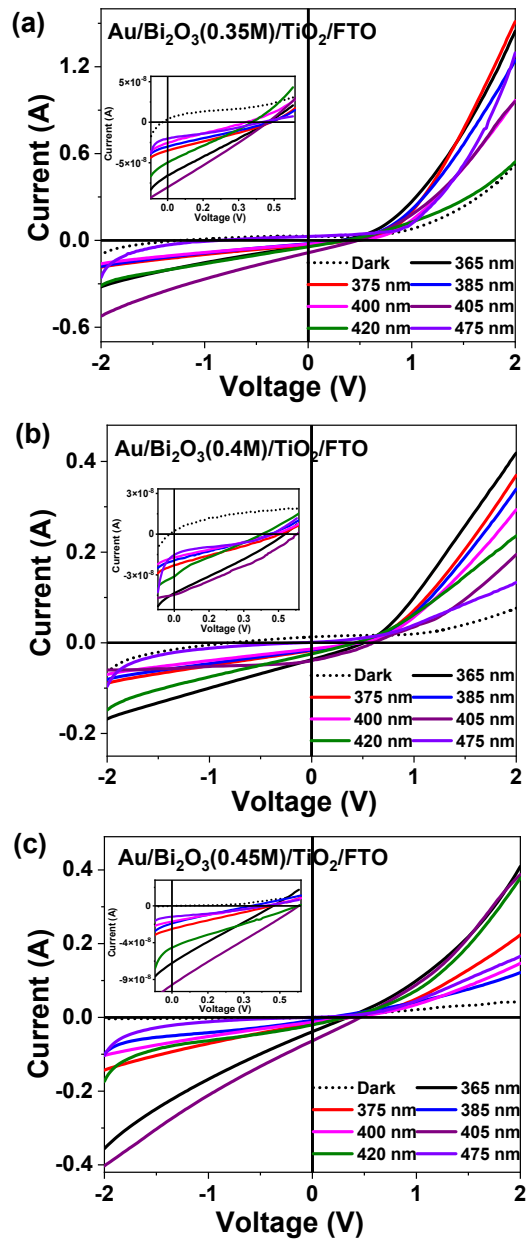


**Fig.S5** I-V curves of (a)  $\text{Bi}_2\text{O}_3(0.35\text{M})/\text{TiO}_2$ , (b)  $\text{Bi}_2\text{O}_3(0.4\text{M})/\text{TiO}_2$  and (c)  $\text{Bi}_2\text{O}_3(0.45\text{M})/\text{TiO}_2$  devices.

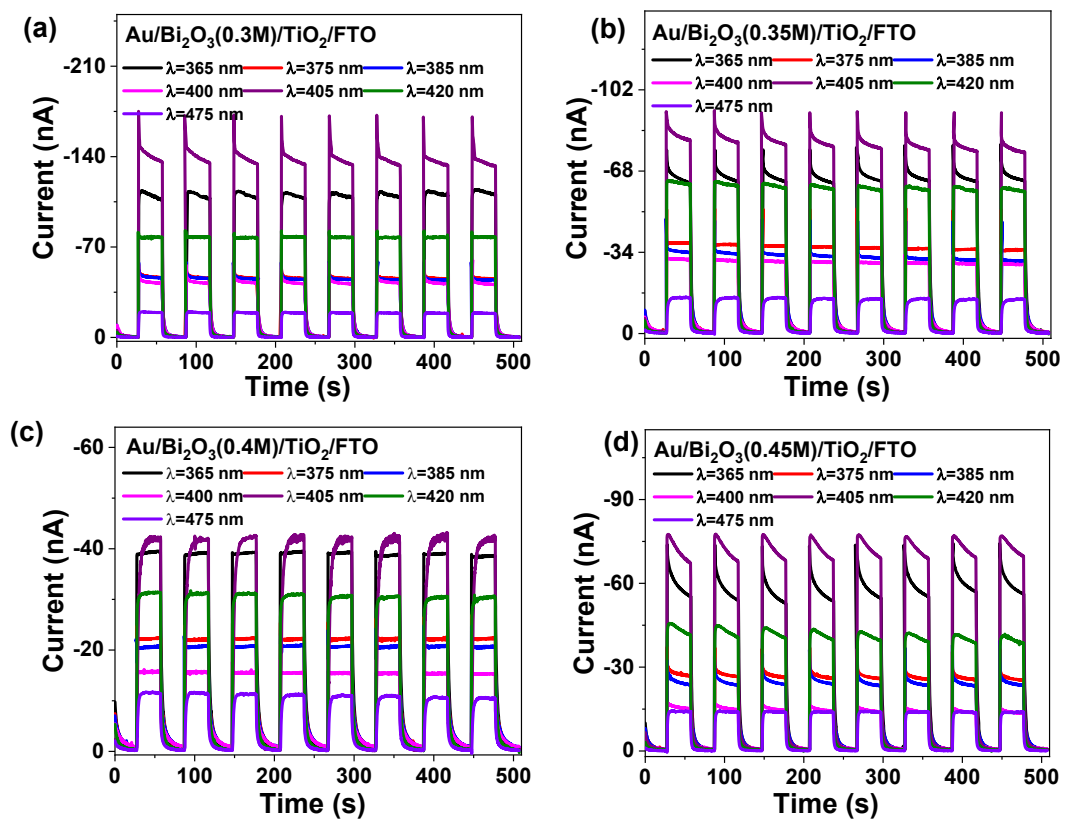


**Fig.S6** I-t curves of (a)  $\text{Bi}_2\text{O}_3(0.3\text{M})/\text{TiO}_2$ , (b)  $\text{Bi}_2\text{O}_3(0.35\text{M})/\text{TiO}_2$ , (c)  $\text{Bi}_2\text{O}_3(0.4\text{M})/\text{TiO}_2$  and (d)  $\text{Bi}_2\text{O}_3(0.45\text{M})/\text{TiO}_2$  devices.

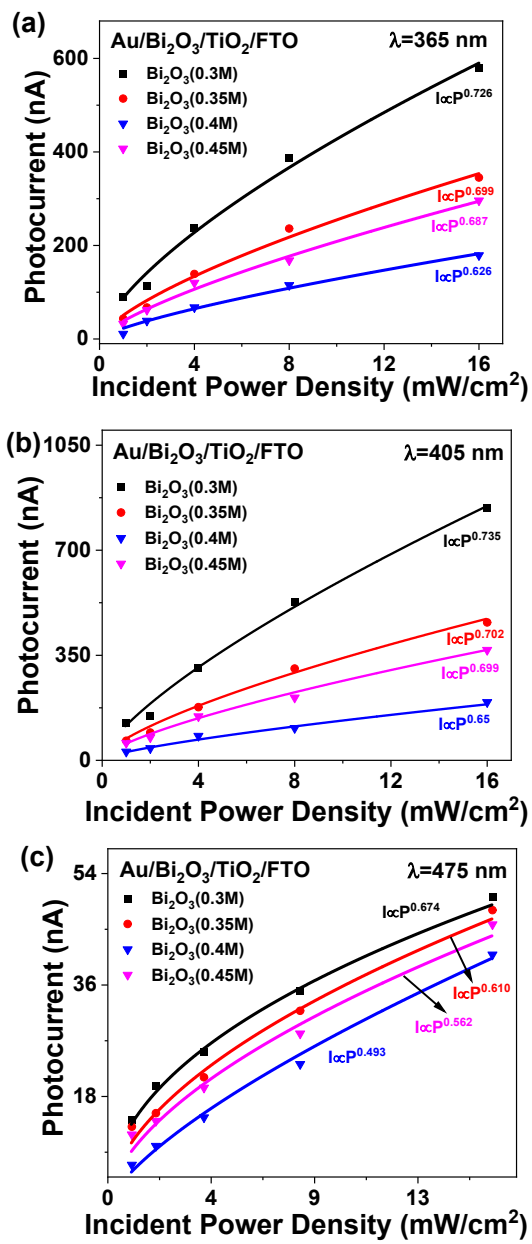


**Fig.S7**  $I_{ph}$  of Au/Bi<sub>2</sub>O<sub>3</sub>/TiO<sub>2</sub>/FTO devices under (a) 365 nm UV light, (b) 405 nm and (c) 475 nm illuminations with different incident powers.

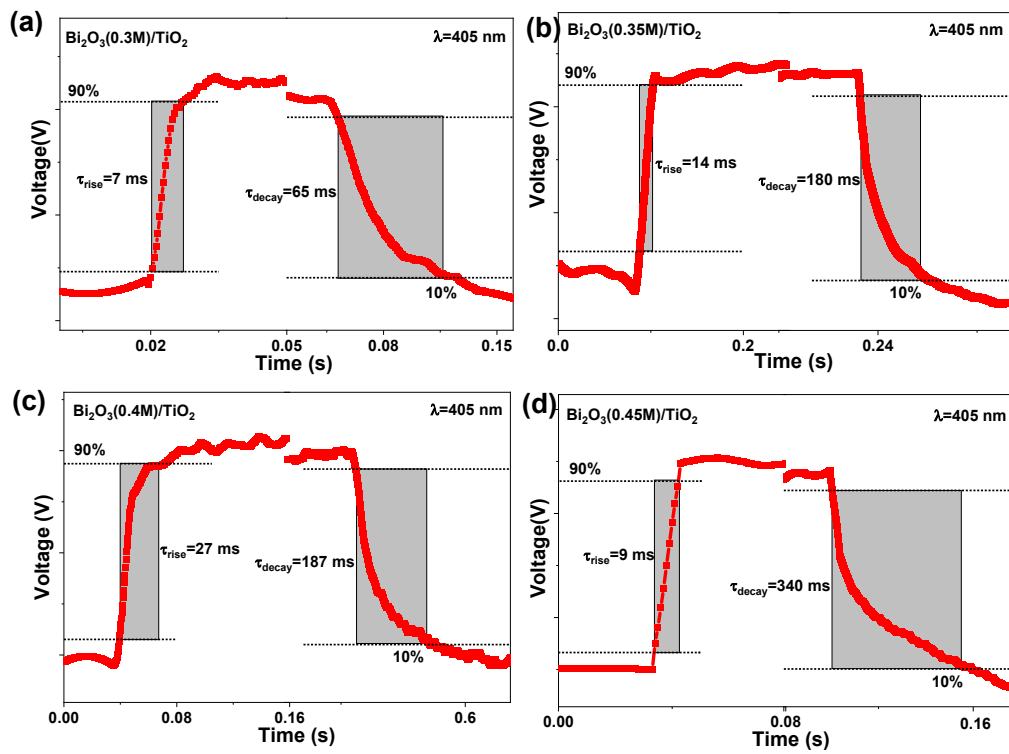


**Fig.S8**  $\tau_{\text{rise}}$  and  $\tau_{\text{decay}}$  of (a)  $\text{Bi}_2\text{O}_3(0.3\text{M})/\text{TiO}_2$ , (b)  $\text{Bi}_2\text{O}_3(0.35\text{M})/\text{TiO}_2$ , (c)  $\text{Bi}_2\text{O}_3(0.4\text{M})/\text{TiO}_2$  and (d)  $\text{Bi}_2\text{O}_3(0.45\text{M})/\text{TiO}_2$  devices at 405 nm light illumination.

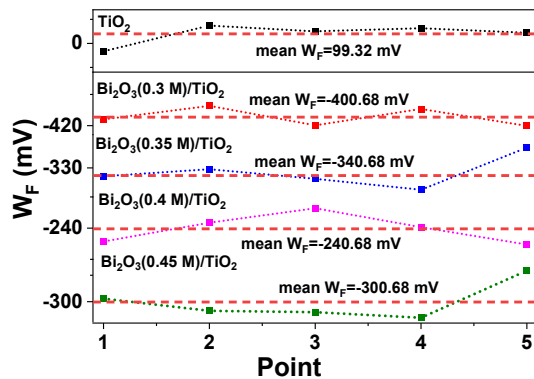


**Fig.S9** Fermi energy level curves obtained from Kelvin probes of  $\text{TiO}_2$  and  $\text{Bi}_2\text{O}_3/\text{TiO}_2$  with different TEA concentrations.

**Table.S1**  $\text{TiO}_2$  and  $\text{Bi}_2\text{O}_3$  films energy band structure related parameters

Samples	$\text{TiO}_2$	$\text{Bi}_2\text{O}_3(0.3\text{M})$	$\text{Bi}_2\text{O}_3(0.35\text{M})$	$\text{Bi}_2\text{O}_3(0.4\text{M})$	$\text{Bi}_2\text{O}_3(0.45\text{M})$
$E_F$ (eV)	-4.46	-4.96	-4.90	-4.80	-4.86
$E_g$ (eV)	3.00	2.42	2.42	2.42	2.42
$E_c$ (eV)	-4.06	-3.36	-3.30	-3.20	-3.26
$E_v$ (eV)	-7.06	-5.73	-5.67	-5.57	-5.63

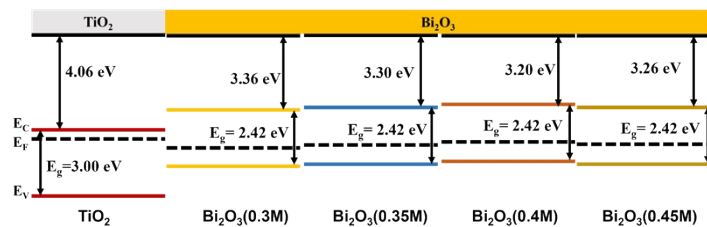


**Fig.S10** Band diagrams before contact of  $\text{Bi}_2\text{O}_3/\text{TiO}_2$  heterojunctions.